



**HAL**  
open science

## Optical and structural properties of SiO<sub>2</sub> co-doped with Si-nc and Er<sup>3+</sup>

Sébastien Cueff, Christophe Labbé, Benjamin Dierre, Julien Cardin, Larysa Khomenkova, Filippo Fabbri, Takashi Sekiguchi, Richard Rizk

► **To cite this version:**

Sébastien Cueff, Christophe Labbé, Benjamin Dierre, Julien Cardin, Larysa Khomenkova, et al.. Optical and structural properties of SiO<sub>2</sub> co-doped with Si-nc and Er<sup>3+</sup>. SPIE NanoScience + Engineering, 2010, San Diego, United States. pp.77660Z, 10.1117/12.865488 . hal-02415361

**HAL Id: hal-02415361**

**<https://hal.science/hal-02415361>**

Submitted on 17 Dec 2019

**HAL** is a multi-disciplinary open access archive for the deposit and dissemination of scientific research documents, whether they are published or not. The documents may come from teaching and research institutions in France or abroad, or from public or private research centers.

L'archive ouverte pluridisciplinaire **HAL**, est destinée au dépôt et à la diffusion de documents scientifiques de niveau recherche, publiés ou non, émanant des établissements d'enseignement et de recherche français ou étrangers, des laboratoires publics ou privés.

# Optical and structural properties of SiO<sub>2</sub> co-doped with Si-nc and Er<sup>3+</sup>

Sébastien Cueff<sup>\*a</sup>, Christophe Labbé<sup>a</sup>, Benjamin Dierre<sup>b</sup>, Julien Cardin<sup>a</sup>, Larysa Khomenkova<sup>a</sup>,  
Filippo Fabbri<sup>b</sup>, Takashi Sekiguchi<sup>b</sup> and Richard Rizk<sup>a</sup>

<sup>a</sup>Centre de Recherche sur les Ions, les Matériaux et la Photonique (CIMAP), ENSICAEN, CNRS,  
CEA/IRAMIS, Université de Caen, 14050 CAEN cedex, France;

<sup>b</sup>Advanced Electronic Materials Center (National Institute for Materials Science, Tsukuba, Japan)

## ABSTRACT

We present a study on erbium-doped silicon rich silicon oxide (SRSO:Er) thin films grown by the magnetron co-sputtering of a three confocal cathodes according to the deposition temperature and the annealing treatment. It is shown that several parameters such as the stoichiometry SiO<sub>x</sub>, the Erbium content and the fraction of agglomerated Silicon are strongly influenced by the deposition temperature. Especially, an increase of the fraction of agglomerated-Si concomitant to a reduction of the erbium content is observed when the deposition temperature is raised. These structural differences have some repercussions on the optical properties that lead to better performances for high-temperature deposited material. It is illustrated by the Er-PL efficiency that is higher for 500°C-deposited than for RT-deposited sample at all annealing temperatures. Finally an investigation of the different emitting centres within the films is performed with a cathodoluminescence technique to highlight the emission of optically-active defect centers in the matrix. It is shown that some oxygen vacancies, namely Silicon-Oxygen Deficient Centers, have a strong contribution around 450-500 nm and are suspected to contribute to the energy transfer towards Er<sup>3+</sup> ions.

**Keywords:** Erbium, Silicon-nanoclusters, thin films, energy transfer, photoluminescence, cathodoluminescence

## 1. INTRODUCTION

The strong enhancement of the Er<sup>3+</sup> emission when coupled to Si nanoclusters (Si-ncs) within a SiO<sub>2</sub> matrix has opened the way for intense research activities [1-4]. Erbium-doped silicon-rich silicon oxide (SRSO:Er) becomes a promising material for integrated photonics, as benefiting from the high and broad-band absorption of Si nanoclusters (Si-nc) to excite indirectly the Er ions [5]. Thanks to this transfer, the effective excitation cross-section of Er<sup>3+</sup> is increased by a factor 10<sup>4</sup> and should permit the use of the erbium 1.5 μm emission for short-haul communication. However, a careful optimization of the material is required to obtain an efficient transfer between Si-nc and Er ions which is strongly dependent on the nm-critical distance separating the Er<sup>3+</sup> ions from the Si-ncs sensitizers [6-8]. It is indeed crucial to nanoengineer the density and distribution of both Er<sup>3+</sup> ions and Si-based sensitizers within the silica matrix. Several groups have analyzed the influence of different annealing treatments on the optical performance of SRSO:Er layers [9-13], usually deposited at room temperature (RT) before being subsequently annealed. Such a process allowed the formation of Si-nc sensitizers and then the observation of Er photoluminescence (PL) under non resonant optical excitation. However, our group has recently observed an Er PL under these indirect excitation conditions on the as-deposited samples at about 500°C [13-15]. The Er emission was improved after annealing at about 600°C, and this aspect was also confirmed by another team on similarly sputtered layers [16]. The observation of Er PL under a non-resonant excitation (476 nm) from the as-deposited samples is indicative of the formation of Si-based sensitizers during the growth process. The purpose of this paper is to investigate the influence of both deposition and annealing temperature on the compositional, structural and optical characteristics of the SRSO:Er layers grown by the magnetron co-sputtering of a three confocal cathodes. The study was made for two typical values of the deposition temperature (Room-Temperature and 500°C) and three annealing temperatures, 600°C, 900°C and 1100°C. The samples were analysed by several techniques: energy dispersive X-ray spectroscopy (EDX), Fourier transform infrared spectroscopy (FTIR), M-lines and photoluminescence (PL) spectroscopy. The samples were also carefully examined by cathodoluminescence (CL) technique with the aim of showing evidence of the variety of emitters present in the samples. A special attention was paid to the centres that can act as sensitizers of Er ions.

\*sebastien.cueff@ensicaen.fr; phone +33(0)2.31.45.26.61;

## 2. EXPERIMENTAL DETAILS

All samples were deposited by the magnetron co-sputtering of a three confocal cathodes. The powers applied on the three cathodes ( $\text{SiO}_2$ , Si and  $\text{Er}_2\text{O}_3$ ) can be independently tuned and each cathode is water-cooled. The applied power densities used for this study are:  $P_{\text{SiO}_2} \approx 8.88 \text{ W/cm}^2$ ,  $P_{\text{Si}} \approx 1.63 \text{ W/cm}^2$ ,  $P_{\text{Er}_2\text{O}_3} \approx 0.44 \text{ W/cm}^2$ . The total plasma pressure during all deposition runs was kept constant at 2 mTorr. The sample holder can be intentionally heated during the deposition and thus the deposition temperature was varied from Room-Temperature (RT) to  $700^\circ\text{C}$  i.e. the maximum temperature that can be applied. The substrate holder is rotated during the growth process, in order to ensure a good homogeneity for both composition and thickness. The duration for all depositions was kept constant at 10h. Some samples were submitted to a ‘post-deposition’ annealing during 1h under a flux of pure nitrogen. The annealing temperature was varied from  $600^\circ\text{C}$  to  $1100^\circ\text{C}$ .

The thickness was determined by M-lines technique. The Er content and the stoichiometry of  $\text{SiO}_x$  matrix were measured by Energy-Dispersive X-ray spectroscopy (EDX). The Fourier Transform InfraRed (FTIR) absorption spectra were recorded under normal incidence to investigate the evolution of the  $\text{TO}_3$  peak. This peak is liable to provide some insights on the structural properties such as the degree of phase separation and Si excess.

Photoluminescence (PL) measurements were carried out using the 476 nm wavelength of an  $\text{Ar}^+$  laser. The spot of the laser beam was carefully determined by a ‘‘moving knife-edge’’ method and was found to be around  $3 \text{ mm}^2$  at  $1/e^2$  of the maximum intensity. For the visible PL assumed to originate from the Si nanoclusters, the emitted light is detected by photomultiplier tube (Hamamatsu). For the Er-related PL in the IR range ( $1.53 \mu\text{m}$ ), the emission is guided through a 1m single-grating monochromator (Jobin Yvon) and collected by a liquid-nitrogen-cooled Germanium detector (Northcoast). All PL measurements were made using the standard lock-in technique with a chopper setting the reference frequency at 9.5 Hz.

Cathodoluminescence (CL) spectra were obtained using a scanning electron microscope (SEM) with CL system under ultra high vacuum system ( $2 \cdot 10^{-10}$  mbar). The electron beam is provided by a Schottky-type field emission electron gun (Omicron) and the beam diameter was around 10 nm. The electron energy and beam current were kept constant at 10 kV and 4 nA, respectively, for the sake of accurate comparison of the different samples. The emitted light of the sample is focused to an optical fiber and guided through the monochromator (Jobin-Yvon Triax 320). The signal is thus detected by a charge coupled device of 2048 channels (CCD, Jobin-Yvon Spectrum One). The excitation time was kept the same (ten seconds) for all samples and the recorded spectra were automatically converted into counts per seconds (cps).

## 3. RESULTS AND DISCUSSION

### 3.1 Compositional characteristics and structural properties

Figure 1 shows the evolution of the thickness, the stoichiometry parameter i.e. the ratio  $x = [\text{O}]/[\text{Si}]$ , and the Er content, in function of the deposition temperature ( $T_d$ ). It appears that the thickness is almost constant for  $T_d \leq 300^\circ\text{C}$ , before decreasing progressively for  $T_d > 300^\circ\text{C}$ . Concerning the composition of the as-deposited samples investigated by EDX, the stoichiometry parameter  $x$  decreases of about 10% when  $T_d$  exceeds  $300^\circ\text{C}$ , reaches a minimum of about 1.4 for  $T_d = 500^\circ\text{C}$ , and then increases slightly. In parallel, the Er content decreases continuously for  $T_d$  higher than  $300^\circ\text{C}$ , by about one order of magnitude when  $T_d$  reaches  $700^\circ\text{C}$ . The change of the layer composition for  $T_d > 300^\circ\text{C}$ , as reflected by the decrease of both Er content and amount of Si excess, is likely due to some temperature-dependent sticking probability of the sputtered elements and the subsequent creation of volatile species assumed to occur for  $T_d > 300^\circ\text{C}$  [17-19]. This suggestion is corroborated by the observed gradual decrease of the thickness against the deposition temperature, as shown in Fig. 1 a).

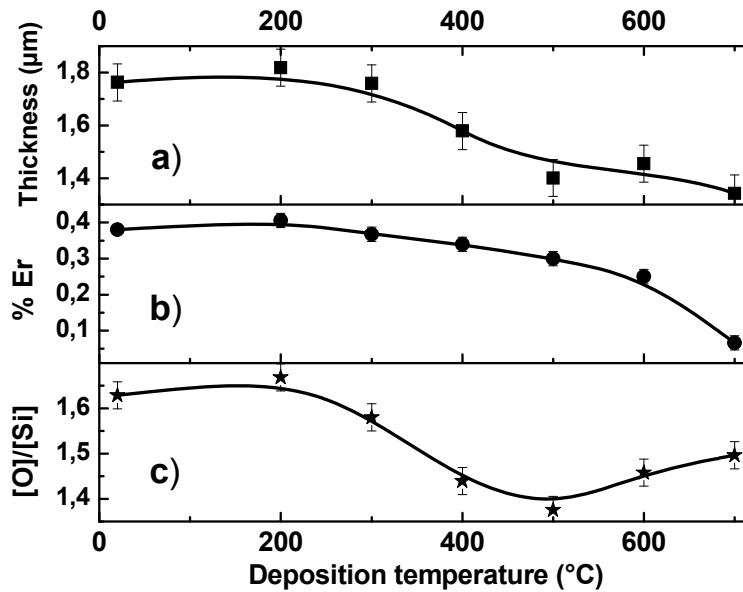


Figure 1. Evolution of different compositional parameters according to the deposition temperature a) thickness as measured by M-Lines, b) atomic percentage of erbium within the deposited films and c) stoichiometric parameter  $x = [O]/[Si]$ .

Besides the already mentioned influence of  $T_d$  on the film composition, one expects also some effect of  $T_d$  on the formation of Si agglomerates that may play the role of sensitizers towards the Er ions. In order to investigate such an effect which will be checked by PL measurements, we recorded FTIR spectra on all as-deposited samples (displayed in Fig. 2), with the aim of examining the shift of the  $TO_3$  peak position with respect to that of stoichiometric silica, allowing a rough estimate of the Si excess [20]. It is based on a linear relationship between the shift of  $TO_3$  peak and the stoichiometry parameter  $y$  of  $SiO_y$ . The linear relationship is:

$$\nu_{TO_3}^{SRSO:Er} = A \cdot y + \nu_{TO_3}^{Si}$$

With

$$A = \frac{\nu_{TO_3}^{Re fSiO_2} - \nu_{TO_3}^{Si}}{2 - 0}$$

The parameter  $y$  can be deduced from:

$$y = 2 \cdot \frac{\nu_{TO_3}^{SRSO:Er} - \nu_{TO_3}^{Si}}{\nu_{TO_3}^{Re fSiO_2} - \nu_{TO_3}^{Si}}$$

Since the FTIR approach allows the detection of only Si bonded to oxygen, the comparison of EDX and FTIR values for the amount of Si excess, enables the determination of the fraction of agglomerated Si.

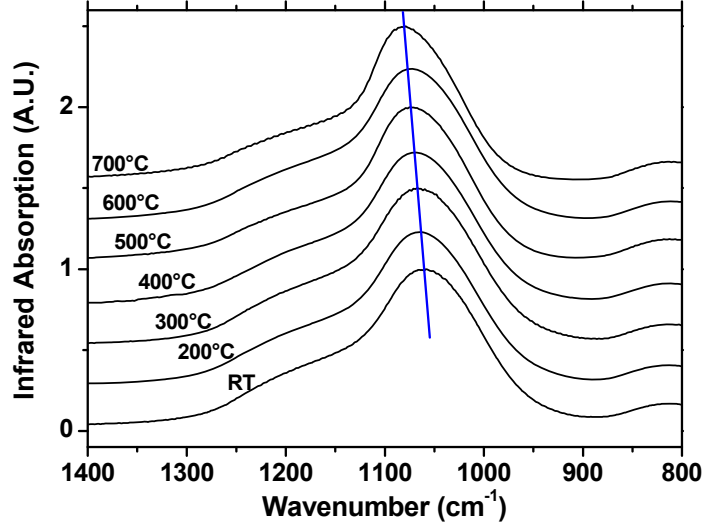


Figure 2. FTIR absorption spectra of the as-deposited samples for all  $T_d$ . The blue line indicates the shift towards high wavenumber when  $T_d$  is raised.

We remind the reader that the  $x$  value corresponding to the stoichiometry of the matrix and measured by EDX (fig.1) is representative of all Si and O atoms. Based on the following relation:



we can estimate the total Silicon-excess given in atomic percent by  $\%Si_{Excess} = [1-x/2]/[1+x]$ . As the FTIR cannot detect the Si atoms linked to other Si atoms within agglomerates, as already mentioned, the estimation of the fraction of agglomerated Silicon can be made using the following relation:



The fraction of agglomerated Si is thus obtained by

$$\%Si_{agglomerated} = 100 \cdot \frac{1 - \frac{x}{y}}{1 + x}$$

The evolution of this fraction against  $T_d$  is compared on figure 3 to that of the total Si excess, as determined by EDX.

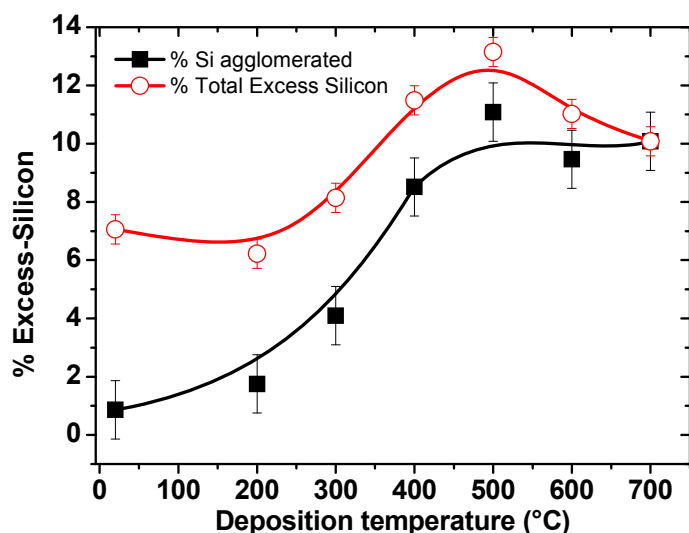


Figure 3. Compared evolution of the total excess-silicon as measured by EDX (empty circles) and the agglomerated excess-silicon (full square).

To note that we are dealing here with the fraction of Si excess whose atoms are linked to each other within Si agglomerates. Such a fraction is obviously different from the number of sensitizers or Si-nc which should be lower than the percentage of Si atoms bonded to only other Si atoms. The former parameter is always lower than the latter one, while both show a clear increase when  $T_d$  is raised beyond 300°C until reaching a maximum for  $T_d = 500^\circ\text{C}$ . The values of both parameters join at about 10% for the highest  $T_d$  value (700°C). At this stage, several observations can be made: (i) increasing the deposition temperature leads to a progressive agglomeration of the Si-excess, (ii) the difference between total Si and agglomerated Si is reducing more and more as  $T_d$  is raised and (iii) at  $T_d = 700^\circ\text{C}$  the agglomerated Si reaches the value of the total excess silicon, indicating a complete phase separation between Si and  $\text{SiO}_2$ .

### 3.2 Photoluminescence spectra

Figure 4 displays the PL spectra obtained under non-resonant excitation wavelength of erbium ions at 476 nm. The upper part presents the PL spectra in the visible range for both RT and 500°C-deposited samples, as-grown and annealed at the indicated temperatures. The lower part of Fig. 4 displays the Er-PL intensity at 1.53  $\mu\text{m}$  for both sets of samples, in function of the annealing temperature. Apart from the interference phenomenon observed for all samples, because of the reflections occurring at the interfaces of these relatively thick (1-1.8 $\mu\text{m}$ ) layers [21], the visible spectrum evolves similarly for both series against the thermal treatment. The emission from the as-deposited is significantly improved after annealing at 600°C for the RT-deposited sample, but much less for that grown at 500°C. However, this visible emission decreases at 900°C before enhancing by about 15-20 times for the samples annealed at 1100°C. Before explaining this behavior, let us examine the evolution against  $T_d$  of the corresponding Er PL which is governed by the excitation of these rare earths through the Si-ncs, leading to a close correlation between both IR (1.54  $\mu\text{m}$ ) and the visible emissions.

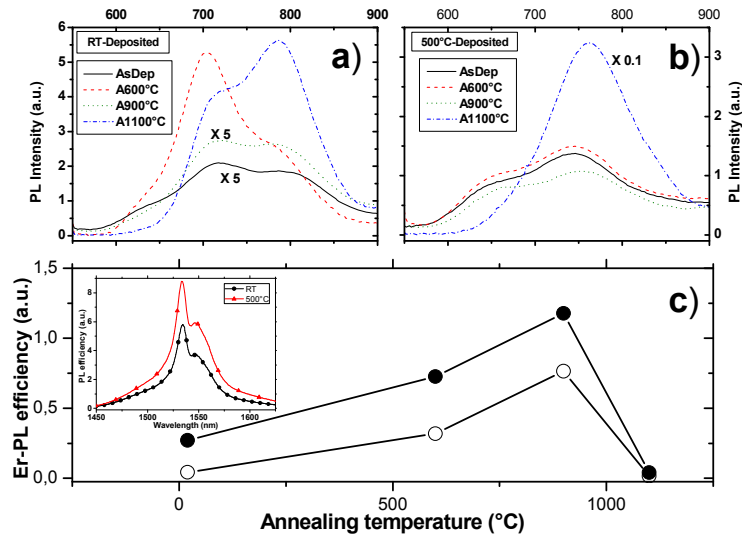


Figure 4. Photoluminescence results on RT-deposited and 500°C-deposited samples. In the upper part are displayed the visible spectra for a) RT-Deposited samples as-deposited and annealed 1h at 600°C, 900°C, 1100°C and b) 500°C deposited samples as-deposited and annealed 1h at 600°C, 900°C and 1100°C. c) Evolution of the Er-PL intensity at 1.53  $\mu\text{m}$  for RT (empty circles) and 500°C-deposited (full circles) samples according to the annealing temperature. Inset: Typical spectra of RT-deposited (black) and 500°C deposited (red) both annealed at 900°C.

To take into account the different values of Er content [Er], Figure 4 c) reports the evolution of the Er-PL efficiency, defined as the ratio  $I_{PL}^{Er} / [\text{Er}]$ ,  $I_{PL}^{Er}$  being the Er PL intensity. It can be seen from Fig. 4 c) that the PL efficiency evolves similarly for both samples in function of  $T_d$ . They both show a gradual increase up to a maximum for  $T_d = 900^\circ\text{C}$ , before collapsing together when  $T_d$  reaches  $1100^\circ\text{C}$ . To note, however, that this PL efficiency is systematically higher for the 500°C-deposited sample. This behavior of Er emission against  $T_d$  was already observed for the emission from as-deposited samples grown at different temperatures [15]. The maximum observed after annealing is around four times higher than that measured for the as-deposited samples. The increase of the PL efficiency is due to an enhanced coupling between the Er ions and the Si-ncs sensitizers whose formation is increasingly favored by the annealing up to  $900^\circ\text{C}$ . The earlier reported increase of the optically active ions with the thermal budget provided an additional support to our explanation [15]. Moreover, the decrease of the visible emission when  $T_a$  is raised from 600 to  $900^\circ\text{C}$ , down to ten times for the RT sample, corroborates our suggestions, inasmuch as the coupled Si-ncs are unable to contribute to the visible emission. For the highest value of  $T_d$  ( $1100^\circ\text{C}$ ), two processes compete to the observed drastic decrease of the PL efficiency: first, the tendency of Er to agglomerates [13, 22], second, the coalescence of Si-nc in large crystallized nanograins, as confirmed by the HRTEM observations of our present samples (not shown).

It is worth noting that, although the samples deposited at two different temperatures show generally similar behaviors, the sample grown at  $500^\circ\text{C}$  shown much better Er emission. The origin of this performance is due to the fact that much more Si-ncs sensitizers are formed during the growth, compared to RT deposited layer. The gap between the samples is approximately maintained after the annealing at different temperature, except the highest one where detrimental effects are occurring.

### 3.3 Cathodoluminescence spectra

Cathodoluminescence provides useful insight on the optically active elements since the incident electron beam is able to excite over a wide range of energy. Thanks to this method, a kind of ‘mapping’ of the different emitting centres can be obtained. It is known that even pure  $\text{SiO}_2$  present CL signals originating from some radiative-defect centers generated by

the imperfect local arrangement of atoms, hence deviating from the perfect  $\text{SiO}_4$  tetraedra. Therefore, to analyse our SRSO:Er samples, it appears essential to compare their CL characteristic to those of sputtered  $\text{SiO}_2$ ,  $\text{SiO}_2$ :Er and SRSO samples. The corresponding CL spectra recorded in the visible range are displayed in figure 5.

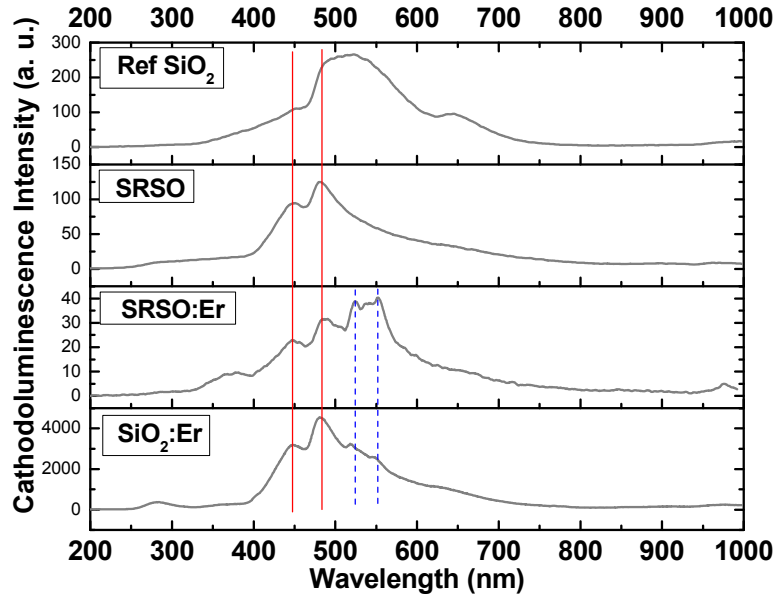


Figure 5. Cathodoluminescence spectra of (from the top to the bottom): a reference  $\text{SiO}_2$ , SRSO sample, SRSO:Er sample and  $\text{SiO}_2$ :Er. All these samples are non-annealed and were deposited at  $500^\circ\text{C}$ .

We can see that the sputtered  $\text{SiO}_2$  layer presents a broad CL spectrum between 300 and 800 nm. This large band is the sum of different contributions, namely Oxygen Vacancies (in this case Oxygen Deficient Center) and Non Bridging Oxygen Hole Centers (NBOHC) [23]. This kind of CL spectrum was already observed by other research groups [24, 25]. When excess-silicon is introduced for the SRSO sample, the corresponding CL spectrum presents two peaks centered at 450 nm and 480 nm, likely to be related to the Oxygen Deficient Center (ODC) [23]. Furthermore, the Si excess in this material is liable to favor the creation of Silicon-ODC (Si-ODC), whereas no emission from NBOHC is detected. When Erbium ions are incorporated for the SRSO:Er sample, the two Si-ODC peaks are still emitting at the exact same wavelengths, in addition to two peaks at 520 nm and 550 nm. As the only difference between this sample and SRSO is the inclusion of  $\text{Er}^{3+}$ , these peaks are likely to come from  $\text{Er}^{3+}$  transitions. This hypothesis is further confirmed by the CL spectra of  $\text{SiO}_2$ :Er which presents the same transitions that are still distinguishable in spite of the wide overlapping of Si-ODC contributions. One can, therefore, argue that these two Er-related emissions are arising from the  $^2\text{H}_{11/2} \Rightarrow ^4\text{I}_{15/2}$  and the  $^4\text{S}_{3/2} \Rightarrow ^4\text{I}_{15/2}$  transitions, respectively. Another important feature deserves to be noted: the Er-related emissions seem to be enhanced by the Si excess in SRSO:Er samples, whereas the Si-ODC contributions decrease by about two orders of magnitude when compared to the corresponding sample free from Si excess. This phenomenon is reminiscent of the earlier mentioned and well known coupling between the Er ions and the Si-based sensitizers. One can therefore consider that we are dealing with a similar energy transfer from Si-ODC towards  $\text{Er}^{3+}$  ions, especially as this is accompanied by a drastic decrease of the emissions from Si-ODC. These centers cannot be, unfortunately, observed in our PL experiment because of the excitation energy used (476 nm), well below that of the Si-ODC absorption band edge at  $\sim 390$  nm. Such emitting centers appear very similar to the so-called Luminescent Centers of Savchyn *et al* [9], which play a predominant sensitizing role towards Er ions.

To check the evolution of emitting centers according to the annealing, we made specific CL analyses on our samples. Figure 6 reports the typical evolution of the CL spectra recorded on the sample as-deposited at  $500^\circ\text{C}$  and those annealed at  $600^\circ\text{C}$ ,  $900^\circ\text{C}$  and  $1100^\circ\text{C}$ .



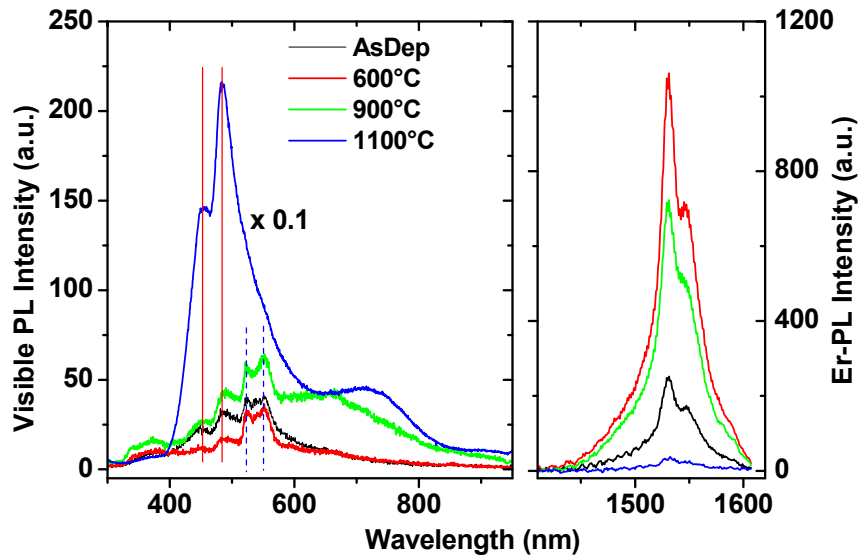


Figure 6. Cathodoluminescence spectra of SRSO:Er samples deposited at 500°C. Each window corresponds to a temperature of annealing.

The CL spectrum in the visible range is slightly less intense after 600°C annealing but show an improvement after 900°C annealing. This latter spectrum shows a quantum-confinement contribution at about ~650 nm due to Si-nc. After an 1100°C annealing the Si-ODCs become predominant, in addition to a strong increase of the quantum-confinement contribution that has redshifted to ~700 nm. This shift can be attributed to the increase of the average size of Si-nc. On the contrary, the 1.5 μm emission of Erbium is almost absent for the highest annealing temperature (1100°C) after showing an optimized emission for 600°C annealing. These counterbalancing behaviors of the emission between Si-based entities (especially SiODC) and Er ions, are indicative of a strong correlation between the presence of Er and the active role of SiODC as emitters and/or sensitizers. It is clear that more studies are necessary to clarify all these aspects, and particularly the role of SiODC in the energy transfer must be investigated. In any case, the emission from those point-defect centers in the visible range, overlapping with Er<sup>3+</sup> and si-nc emission, strongly suggest that they may take part in the sensitization of Er ions.

## CONCLUSION

The optical and structural properties of erbium-doped silicon rich silicon oxide (SRSO:Er) thin films grown by magnetron co-sputtering were investigated according to the deposition temperature and the annealing treatment. The temperature of deposition was shown to have several crucial effects on the properties of the deposited thin film. When the deposition temperature is raised, an increase of the fraction of agglomerated Si is observed concomitantly to a lowering of the Er content. As a consequence, the 500°C-deposited sample present a systematically higher Er-PL efficiency than the RT-deposited sample and this, for all temperature of annealing. Optimized conditions for PL were found to be a deposition temperature of 500°C and an annealing temperature of 900°C. To note that both the 700°C-deposition and the 1100°C-annealing were demonstrated to have detrimental effects on the energy transfer from si-nc to Er<sup>3+</sup>. The cathodoluminescence technique was used to investigate the emission of optically-active defect centers that cannot be excited by the wavelength used in PL (476 nm). It was shown that Silicon-Oxygen Deficient Centers, have a strong luminescence around 450-500 nm and are suspected to contribute to the energy transfer towards Er<sup>3+</sup> ions. Further experiment needs to be carried out in order to deeper investigate an eventual sensitizing role of Si-ODC towards Er<sup>3+</sup> ions.

## REFERENCES

- [1] A. J. Kenyon, P. F. Trwoga, M. Federighi, and C. W. Pitt, "Optical properties of PECVD erbium-doped silicon-rich silica: evidence for energy transfer between silicon microclusters and erbium ions," *J. Phys.:Condens. Matter* **6**, L319 (1994).
- [2] M. Fujii, M. Yoshida, Y. Kanzawa, S. Hayashi and K. Yamamoto, "1.54  $\mu\text{m}$  photoluminescence of Er doped into SiO films containing Si nanocrystals: Evidence for energy transfer from Si nanocrystals to Er," *Appl. Phys. Lett.* **71**, 1198 (1997).
- [3] G. Franzò, V. Vinciguerra, and F. Priolo, "The excitation mechanism of rare-earth ions in silicon nanocrystals," *Appl. Phys.A: Mater. Sci. Process* **3**, 69 (1999).
- [4] F. Gourbilleau, M. Levalois, C. Dufour, J. Vicens, and R. Rizk, "Optimized conditions for an enhanced coupling rate between Er ions and Si nanoclusters for an improved 1.54- $\mu\text{m}$  emission," *J. Appl. Phys.* **95**, 3717 (2004).
- [5] J. Lee, J.H. Shin, and N. Park, "Optical gain at 1.5  $\mu\text{m}$  in nanocrystal Si-sensitized Er-doped silica waveguide using top-pumping 470 nm LEDs," *J. Lightwave Technol.* **23**, 19 (2005).
- [6] J.H. Jhe, J. H. Shin, K. J. Kim, and D. W. Moon, "The characteristic carrier-Er interaction distance in Er-doped a-Si/SiO superlattices formed by ion sputtering," *Appl. Phys. Lett.* **82**, 4489 (2003).
- [7] B. Garrido, C. Garcia, P. Pellegrino, D. Navarro-Urrios, N. Dalbosso, L. Pavesi, F. Gourbilleau, and R. Rizk, "Distance dependent interaction as the limiting factor for Si nanocluster to Er energy transfer in silica," *Appl. Phys. Lett.* **89**, 163103 (2006).
- [8] F. Gourbilleau, C. Dufour, R. Madelon, and R. Rizk, "Effects of Si nanocluster size and carrier-Er interaction distance on the efficiency of energy transfer," *J. Lumin.* **126**, 581 (2007).
- [9] O. Savchyn, F. R. Ruhge, P. G. Kik, R. M. Todi, K. R. Coffey, H. Nukala, and H. Heinrich, "Luminescence-center-mediated excitation as the dominant Er sensitization mechanism in Er-doped silicon-rich SiO<sub>2</sub> films," *Phys. Rev. B* **76**, 195419 (2007).
- [10] G. Wora Adeola, H. Rinnert, P. Miska, and M. Vergnat, "Influence of the annealing temperature on the photoluminescence of Er-doped SiO thin films," *J. Appl. Phys.* **102**, 053515 (2007).
- [11] A. Kanjilal, L. Rebohle, M. Voelskow, W. Skorupa, and M. Helm, "Influence of the annealing on the Er luminescence in Si-rich SiO<sub>2</sub> layers coimplanted with Er ions," *J. Appl. Phys.* **104**, 103522 (2008).
- [12] A. R. Wilkinson and R. G. Elliman, "The effect of annealing environment on the luminescence of silicon nanocrystals in silica," *J. Appl. Phys.* **96**, 4018 (2004).
- [13] S. Cueff, C. Labbé, J. Cardin and R. Rizk, "Impact of the annealing temperature on the optical performances of Er-doped Si-rich silica systems," *IOP Conf. Ser.: Mater. Sci. Eng. B* **6**, 012021 (2009).
- [14] K. Hijazi, R. Rizk, J. Cardin, L. Khomenkova, and F. Gourbilleau, "Towards an optimum coupling between Er ions and Si-based sensitizers for integrated active photonics," *J. Appl. Phys.* **106**, 024311 (2009)
- [15] S. Cueff, C. Labbé, J. Cardin, J-L. Doualan, L. Khomenkova, K. Hijazi, O. Jambois, B. Garrido and R. Rizk, "Efficient energy transfer from Si-nanoclusters to Er ions in silica induced by substrate heating during deposition," *J. Appl. Phys.* (to be published)
- [16] O. Savchyn R. M. Todi, K. R. Coffey, L. K. Ono, B. R. Cuenya, and P. G. Kik, "Excitation wavelength independent sensitized Er concentration in as-deposited and low temperature annealed Si-rich SiO films," *Appl. Phys. Lett.* **95** 231109 (2009)
- [17] Wickboldt, "Luminescence from SiO<sub>x</sub> nanoclusters," *Mat. Res. Soc. Symp. Proc. Vol. 358* (1995)
- [18] Y. Takakuwa, M. Nihei, and N. Miyamoto, "Outdiffusion and Subsequent Desorption of Volatile SiO Molecules during Annealing of Thick SiO<sub>2</sub> Films in Vacuum," *Jpn. J. Appl. Phys., Part 2* **32**, L480 (1993).
- [19] D. Gautam, E. Koyanagi and T. Uchino, "Photoluminescence properties of SiO<sub>x</sub> thin films prepared by reactive electron beam evaporation from SiO and silica nanoparticles," *J. Appl. Phys.*, **105**, 073517 (2009).
- [20] P.G. Pai, S.S. Chao, Y. Takagi, and G. Lukovsky, "Infrared spectroscopic study of SiO<sub>x</sub> films produced by plasma enhanced chemical vapor deposition," *J. Vac. Sci. Tech. A4*, 689 (1986)
- [21] R. Ferre, B. Garrido, P. Pellegrino, M. Peralvarez, C. Garcia, J. A. Moreno, J. Carreras, and J. R. Morante, "Optical-geometrical effects on the photoluminescence spectra of Si nanocrystals embedded in SiO<sub>2</sub>," *J. Appl. Phys.* **98**, 084319 (2005)
- [22] A. Polman, D. C. Jacobson, D. J. Eaglesham, Ft. C. Kistler, and J. M. Poate, "Optical doping of waveguide materials by MeV Er implantation," *J. Appl. Phys.* **70** (1991)

- [23] L. Skuja, "Optically active oxygen-deficiency-related centers in amorphous silicon dioxide," *J. non-cryst. Sol.* 239, 16-48, (1998)
- [24] H. Koyama, "Cathodoluminescence study of SiO<sub>2</sub>," *J. Appl. Phys.* 51 (1980)
- [25] H.-J. Fitting, "How to make silica luminescent?," *J. Lum.*, 129, 1488-1492 (2009)